Inorganic Chemistry

Article

pubs.acs.org/IC

# Reactivity of Cr(III) μ-Oxo Compounds: Catalyst Regeneration and Atom Transfer Processes

K. Cory MacLeod,[†] Brian O. Patrick,[‡] and Kevin M. Smith*,[†]

[†]Department of Chemistry, University of British Columbia Okanagan, 3333 University Way, Kelowna, BC, Canada V1V 1V7

[‡]Department of Chemistry, University of British Columbia, Vancouver, British Columbia, Canada V6T 1Z1

Supporting Information

**ABSTRACT:** Oxidation of CpCr[(XylNCMe)$_2$CH] (Xyl = 2,6-Me$_2$C$_6$H$_3$) with pyridine *N*-oxide or air generated the μ-oxo dimer, {CpCr[(XylNCMe)$_2$CH]}$_2$(μ-O). The μ-oxo dimer was converted to paramagnetic Cr(III) CpCr[(XylNCMe)$_2$CH](X) complexes (X = OH, O$_2$CPh, Cl, OTs) via protonolysis reactions. The related Cr(III) alkoxide complexes (X = OCMe$_3$, OCMe$_2$Ph) were prepared by salt metathesis and characterized by single crystal X-ray diffraction. The interconversion of the Cr(III) complexes and their reduction back to Cr(II) with Mn powder were monitored using UV−vis spectroscopy. The related CpCr[(DepNCMe)$_2$CH] (Dep = 2,6-Et$_2$C$_6$H$_3$) Cr(II) complex was studied for catalytic oxygen atom transfer reactions with PPh$_3$ using O$_2$ or air. Both Cr(II) complexes reacted with pyridine *N*-oxide and γ-terpinene to give the corresponding Cr(III) hydroxide complexes. When CpCr[(DepNCMe)$_2$CH] was treated with pyridine *N*-oxide in benzene in the absence of hydrogen atom donors, a dimeric Cr(III) hydroxide product was isolated and structurally characterized, apparently resulting from intramolecular hydrogen atom abstraction of a secondary benzylic ligand C−H bond followed by intermolecular C−C bond formation. The use of very bulky hexaisopropylterphenyl ligand substituents did not preclude the formation of the analogous μ-oxo dimer, which was characterized by X-ray diffraction. Attempts to develop a chromium-catalyzed intermolecular hydrogen atom transfer process based on these reactions were unsuccessful. The protonolysis and reduction reactions of the μ-oxo dimer were used to improve the previously reported Cr-catalyzed radical cyclization of a bromoacetal.

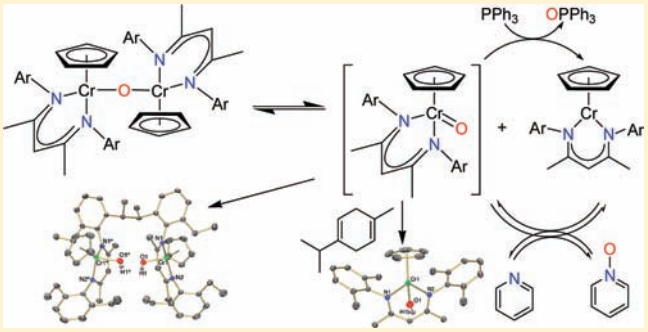


## INTRODUCTION

The use of first-row transition metals is becoming more common in catalytic C−C bond forming reactions for organic synthesis.[1] Compared to their heavier congeners, first-row metal complexes are cheaper and often exhibit complementary reactivity, but they also have a recognized propensity to engage in radical reactivity.[2] Redox noninnocent ligands have been employed to enforce two-electron chemistry.[3] Alternatively, applications have been developed that explicitly harness the metal center's ability to engage in single-electron transfer reactivity.[4] We have been using well-defined cyclopentadienyl chromium β-diketiminate complexes to investigate the reactivity of Cr(II) and Cr(III) complexes.[5] Oxidative addition of organic halides, RX, with the Cr(II) compound CpCr[(XylNCMe)$_2$CH] (**1**) gives a 1:1 mixture of the Cr(III) halide and Cr(III) alkyl complexes.[6] Use of excess RX and PbX$_2$-activated manganese as a stoichiometric reductant of CpCr[(XylNCMe)$_2$CH](X), where X = Br or Cl (**2**) provides a convenient synthetic route to CpCr[(XylNCMe)$_2$CH](R) alkyls. We have applied this reactivity to the catalytic radical cyclization of haloacetals (eq 1).[7]

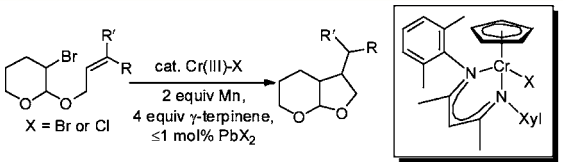


(1)

The paramagnetic Cr(III) halide complexes are air-stable as crystalline solids that can be stored in air for years without any apparent decomposition, and even CpCr[(XylNCMe)$_2$CH](R) alkyl complexes can be remarkably resistant to O$_2$ if protected from ambient light.[8] However, similar to most reduced metal complexes capable of single-electron oxidative addition of relatively strong carbon−halogen bonds,[9,10] these Cr(II) compounds are highly air-sensitive. The CpCr[(XylNCMe)$_2$CH] system would be more generally applicable if its tolerance to air and other impurities in substrates and solvents could be improved.

In this paper, we examine the problem of air-sensitivity in the radical reactivity of CpCr[(ArNCMe)$_2$CH] using stoichiometric manganese as a reductant. The product of air oxidation of CpCr[(XylNCMe)$_2$CH], **1**, is the Cr(III) μ-oxo complex **3**.[11−13] Although both the Cp and β-diketiminate ligands

**Received:** October 14, 2011
**Published:** December 16, 2011

   dx.doi.org/10.1021/ic202233f | *Inorg. Chem.* 2012, 51, 688−700

remain intact and Cr-bound in **3**, the Cr(III)−O bonds were expected to pose a significant obstacle to reforming the reactive Cr(II) complex, **1** (Scheme 1). We report the conversion of the

**Scheme 1**

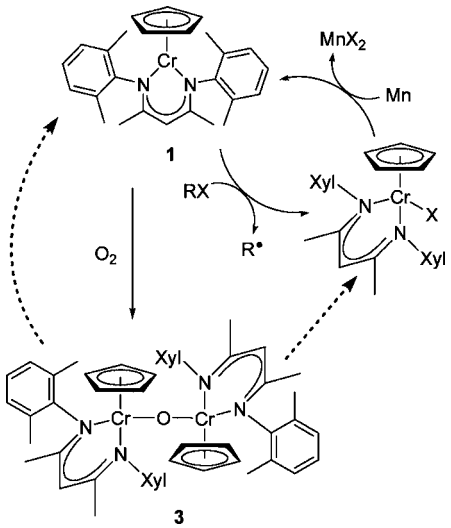


$\mu$-oxo product to other Cr(III) species more amenable to reduction to Cr(II) under catalytically relevant conditions, including the independent synthesis, spectroscopic characterization, and structural elucidation of these Cr(III) species. The scope of manganese reactivity with Cr(III) species was examined as well as catalyst regeneration of the $\mu$-oxo complex **3** for haloacetal cyclization. The $\beta$-diketiminate ligand was modified to discourage $\mu$-oxo formation, leading to examination of the reactivity of a putative Cr(IV) oxo intermediate. Catalytic conditions for $PPh_3$ oxidation by oxygen atom transfer with $O_2$ or air as oxygen atom sources, and intra- and intermolecular hydrogen atom transfer (HAT) reactivity is also presented.

## RESULTS AND DISCUSSION

**Synthesis of {CpCr[(XylNCMe)$_2$CH]}$_2$($\mu$-O).** The Cr(III) $\mu$-oxo complex {CpCr[(XylNCMe)$_2$CH]}$_2$($\mu$-O), **3**, was prepared by reaction of the Cr(II) complex **1** with $^1/_2$ equiv of pyridine *N*-oxide under an inert atmosphere in hexanes. Upon stirring overnight, the precipitate was isolated and dried to provide **3** as an analytically pure orange powder in high yield. Complex **3** exhibits a strong absorbance peak in the UV−vis spectrum with $\lambda_{max}$ = 362 nm ($\varepsilon$ = 20700 $M^{-1}$ $cm^{-1}$) and a shoulder at 471 nm. The solution magnetic moment of 2.39 $\mu_B$ for compound **3** is significantly lower than expected for two high-spin Cr(III) metal centers. Similar antiferromagnetic coupling was observed for the Cr(III) $\mu$-oxo compound [{Cr(NCS)(TPyEA)}$_2$O] ($\mu_{eff}$ = 1.63 $\mu_B$/Cr atom),[11a] as well as the chromium porphyrin heterobimetallic compounds (py)(TPP)CrOFe(tmtaa) and (Tpp)CrOFe(Pc) ($\mu_{eff}$ = 3.51 $\mu_B$/molecule and 3.12 $\mu_B$/molecule, respectively).[14]

Crystallographic analysis of compound **3** confirmed the presence of the $\mu$-oxo core (Figure 1), with a Cr−O−Cr angle of 174.5(2)° and Cr−O bond lengths of 1.834(3) Å, similar to the previously reported [{Cr(NCS)(TPyEA)}$_2$O] (Cr−O−Cr = 176.5(6)° and Cr−O bond lengths of 1.82(1) and 1.81(1) Å.[11a] The solid-state molecular structure exhibits a staggered type of arrangement for the Cp and $\beta$-diketiminate ligands, where $^1/_2$ of the molecule is rotated approximately 143° with

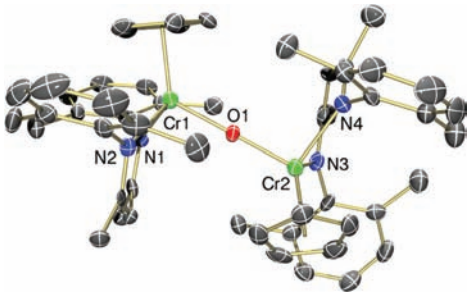


**Figure 1.** Thermal ellipsoid diagram (50%) of **3**. $^1/_2$ Molecule of hexanes and all H atoms are omitted for clarity.

respect to the other. The staggered geometry of the ligands is presumably a result of steric strain in the molecule due to the xylyl ortho-methyl groups of the $\beta$-diketiminate ligands, which also exhibit elongation of the Cr−N bonds (2.046−2.055 Å), a trend previously observed with only the most sterically encumbered trivalent CpCr[(ArNCMe)$_2$CH](R) alkyl compounds.[8]

Air exposure of a solution of Cr(II) complex **1** resulted in a rapid color change from green to orange, with a UV−vis spectrum that matched that of the $\mu$-oxo compound **3**. Attempts to determine the rate of reaction of $O_2$ with compound **1** were unsuccessful, as the reaction of a 9.8 × $10^{-5}$ M solution of **1** with 10 equiv of dry $O_2$ went to completion shortly after mixing (<5 s). Previous work by Liston and West reported the formation of a Cr(III) $\mu$-oxo porphyrin species from oxidation of Cr(II) porphyrins with oxygen (Scheme 2).[15] They proposed that the first step involved the

**Scheme 2**

$$Cr(II) + O_2 \rightleftharpoons Cr(III)(O_2)$$
$$Cr(III)(O_2) + Cr(II) \longrightarrow Cr(III)(O_2)Cr(III)$$
$$Cr(III)(O_2)Cr(III) \longrightarrow 2Cr(IV)O$$
$$Cr(IV)O + Cr(II) \rightleftharpoons Cr(III)OCr(III)$$

formation of a Cr(III) superoxo species that was subsequently trapped by another equiv of Cr(II) porphyrin. This intermediate then undergoes O−O bond cleavage forming two Cr(IV) oxo porphyrin compounds, which were found to react reversibly in solution with the Cr(II) porphyrin starting material to form a Cr(III) $\mu$-oxo porphyrin complex. Veige and co-workers also reported the formation of a Cr(IV) $\mu$-oxo compound by a Cr(III)/Cr(V) redox couple analogous to the Cr(II)/Cr(IV) couple proposed in Scheme 2.[11f]

The reaction of the Cr(II) compound **1** with pyridine *N*-oxide under air-free conditions provides a cleaner route for the isolation of $\mu$-oxo compound **3**. Although compound **3** was the product of air oxidation of **1**, a subsequent color change from orange to green was observed over several hours when solutions of **3** were subjected to air exposure.

**Reactivity of {CpCr[(XylNCMe)$_2$CH]}$_2$($\mu$-O).** Attempts to further oxidize the Cr(III) $\mu$-oxo compound **3** to a higher valence Cr oxo species were not successful. The reaction of the Cr(II) complex **1** with an excess of pyridine *N*-oxide did not affect the formation of **3** as the sole isolable product (Scheme 3, path A).[16] In addition, **3** was unreactive toward a >10-fold excess of pyridine *N*-oxide in a variety of solvents under an inert atmosphere over a two day period.


dx.doi.org/10.1021/ic202233f | Inorg. Chem. 2012, 51, 688−700

**Scheme 3**

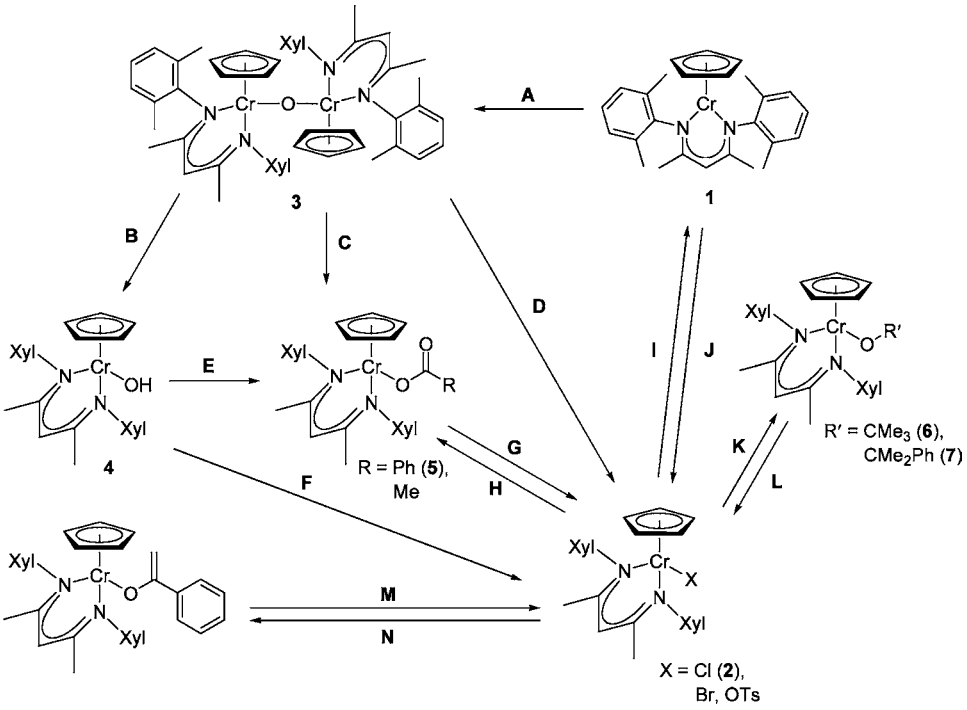


**Scheme 4**

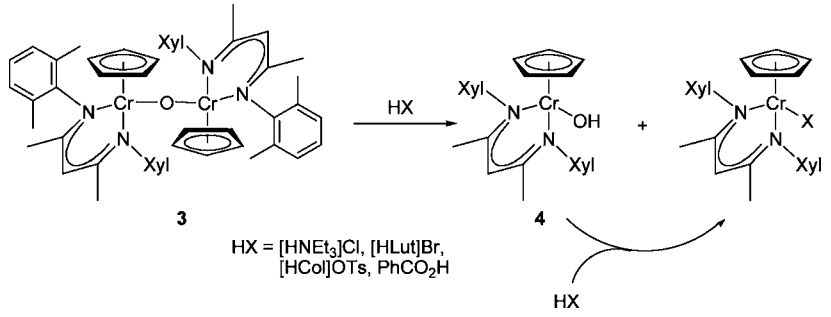


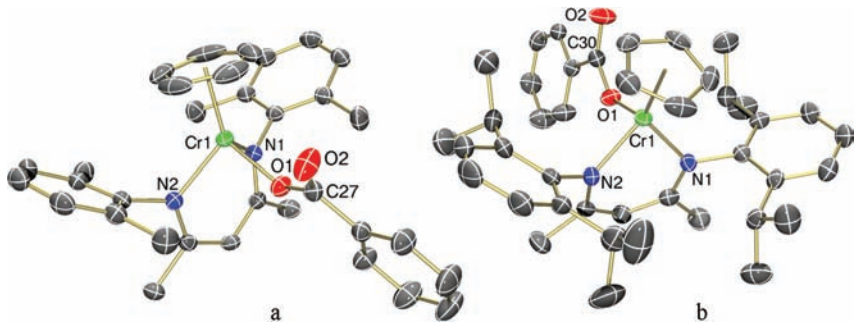


**Figure 2.** Thermal ellipsoid diagrams (50%) of (a) **5** and (b) **5a**. All H atoms are omitted for clarity.

We found that atmospheric moisture was responsible for the air-sensitivity of complex **3**. Under an inert atmosphere, complex **3** reacted with a stoichiometric amount of degassed water to affect the color change previously observed for the prolonged air exposure of **3** (Scheme 3, path B). The UV–vis spectrum exhibits a strong absorption at 390 nm and two weaker absorptions at 506 and 611 nm. Characterization of this green species confirmed that the water had protonated the $\mu$-oxo ligand of **3** to produce 2 equiv of a Cr(III) hydroxide compound CpCr[(XylNCMe)$_2$CH](OH), **4**.

The $\mu$-oxo complex **3** was found to react cleanly with a variety of proton sources HX, where HX = [HNEt$_3$]Cl, [HLut]Br, [HCol]OTs, PhCO$_2$H (Lut = lutidine, 2,6-dimethylpyridine; Col = collidine, 2,4,6-trimethylpyridine), generating the monometallic Cr(III) complexes shown in Scheme 3, paths C and D. The addition of 2 equiv of acid in path D cleanly generated 2 equiv of the corresponding


dx.doi.org/10.1021/ic202233f | Inorg. Chem. 2012, 51, 688–700

Cr(III)−X complex, where X = Cl (**2**), Br, or OTs. Additionally, the reaction of **3** with 2 equiv of benzoic acid yielded the Cr(III) benzoate complex CpCr[(XylNCMe)$_2$CH](O$_2$CPh), **5**, in 66% isolated yield (Scheme 3, path C).

The clean conversion of the $\mu$-oxo complex **3** to the Cr(III) halide and benzoate complexes prompted further investigation (Scheme 3, paths C and D). Reacting isolated Cr(III) hydroxide **4** with the HX sources under the same reaction conditions as complex **3** led to the clean formation of the Cr(III)−X compounds (Scheme 3, paths E and F). This result suggests that the reaction of **3** with HX proceeds by an initial reaction of **3** with 1 equiv of HX to form the Cr(III)−X product and a stoichiometric amount of the hydroxide species **4**, which then reacts with a second equiv of HX to produce a second equiv of Cr(III)−X and 1 equiv of water (Scheme 4). Notably, isolation of the Cr(III)−X compounds did not appear to be hindered by the stoichiometric amount of water presumably generated as the byproduct of the reaction.

**Independent Synthesis and Characterization of CpCr[(ArNCMe)$_2$CH](X).** The benzoate complex **5** was independently synthesized in good yield by reaction of the Cr(III) chloride complex **2** with silver benzoate (Scheme 2, path H). Compound **5** has a strong absorption in the UV−vis spectrum at 413 nm and two weaker absorptions at 503 and 584 nm and was structurally characterized by X-ray crystallography (Figure 2a).

In addition to preparing the benzoate complex **5** by salt metathesis from the chloride precursor **2**, we previously reported the synthesis of the acetate analogue CpCr[(XylNCMe)$_2$CH](O$_2$CMe) from compound **2** and AgO$_2$CMe.[17] A Cr(III) benzoate species was also prepared from the more sterically hindered (DppNCMe)$_2$CH ligand, where Dpp =2,6-$^i$Pr$_2$C$_6$H$_3$, by single electron oxidation of the Cr(II) precursor, CpCr[(DppNCMe)$_2$CH], with 1 equiv of silver benzoate (Figure 2b). Somewhat surprisingly, CpCr[(DppNCMe)$_2$CH](O$_2$CPh), **5a**, displays a Cr−O bond length that does not differ significantly from that of **5** or the previously reported acetate complex (see Table 1). Conversely, the Cr−N bonds of **5a** appear to lengthen slightly, compared to the other two compounds, as a means of alleviating steric strain in the molecule, a feature also observed with the $\mu$-oxo compound **3**. The Cr−O−C angle in the two benzoate compounds is ∼4° larger than that of the acetate analogue, owing to the increased steric requirements of the benzoate ligand.

**Table 1. Selected Bond Lengths (Å) and Bond Angles (deg) for Complexes CpCr[(XylNCMe)$_2$CH](O$_2$CMe), 5, and 5a**

| | CpCr[(XylNCMe)$_2$CH](O$_2$CMe) | 5 | 5a |
|---|---|---|---|
| Cr−N(1) | 2.010(5) | 2.0079(14) | 2.0233(18) |
| Cr−N(2) | 2.004(6) | 2.0125(14) | 2.0359(19) |
| Cr−O(1) | 1.952(5) | 1.9355(12) | 1.9309(15) |
| O(1)−C | 1.278(9) | 1.286(2) | 1.299(3) |
| O(2)−C | 1.230(9) | 1.221(2) | 1.227(3) |
| O(1)−C−O(2) | 124.9(7) | 125.69(16) | 126.0(2) |
| O(1)−C−C | 115.2(7) | 113.82(14) | 113.3(2) |
| O(2)−C−C | 119.9(7) | 120.49(15) | 120.7(2) |
| Cr−O(1)−C | 133.6(5) | 138.26(11) | 137.99(15) |

The Cr(III) alkoxide compounds CpCr[(XylNCMe)$_2$CH](OR), where R = CMe$_3$ (**6**) or CMe$_2$Ph (**7**), were prepared by salt metathesis of the Cr(III) chloride compound, **2**, with the appropriate potassium alkoxide (Scheme 3, path K). Both alkoxide compounds **6** and **7** have similar UV−vis spectra with absorption bands at 395, 490, and 730 nm. The solid-state molecular structures of **6** and **7** (Figure 3) display relatively large Cr−O−C bond angles of 151.8(2)° and 149.0(1)°, respectively, to accommodate the large *tert*-butyl and CMe$_2$Ph groups of the alkoxide ligands. The Cr−N bond lengths for compounds **6** and **7** (2.011(2)−2.039(2) Å) are similar to the other Cr(III) compounds reported herein, despite the sterically demanding alkoxide ligands, highlighting the importance of the flexibility of the Cr−O−C bond angle in accommodating the large alkoxide group. The Cr−O bond lengths of **6** and **7** (1.867(2) and 1.879(1) Å, respectively) are similar to the octahedral Cr(III) alkoxide compounds [Cp′Cr(OAr)Cl]$_2$, where Cp′ = C$_5$H$_5$ or C$_5$Me$_5$ and Ar = 2,6-$^i$Pr$_2$C$_6$H$_3$) with Cr−O bond lengths of 1.869(2) and 1.893(1) Å.[18]

**Manganese Reactivity with Cr(III)-X.** The oxophilicity of early first-row metals presents a challenge for catalyst design when these strong M−O bonds must be broken to reform reactive low-valent species. The reducing agents selected must also be compatible with the organic substrates, their functional groups, and the other reagents in the reaction mixture. A particularly effective strategy developed by Fürstner uses a multicomponent system with a first-row transition metal catalyst, stoichiometric reductant, and Me$_3$SiCl.[19] This system is useful with TiCl$_3$ for carbonyl coupling reactions, normally limited to stoichiometric transformations because of the strong Ti−O bonds formed, now rendered catalytic with Me$_3$SiCl providing the thermodynamic driving force to cleave the Ti−O bond, with the resulting Ti halide species being reduced with Zn powder.[20] This system was later extended to a chromium-catalyzed Nozaki−Hiyama−Kishi (NHK) reaction using Mn as the stoichiometric reductant of choice as it is inexpensive, exhibits very limited reactivity with typical organic halides and their functional groups, and the Mn halide by-products are only weakly Lewis acidic.[21,22] In their development of asymmetric NHK catalysts, Cozzi and co-workers noted that Me$_3$SiCl activated the Mn, accelerating the reduction of CrCl$_3$ to Cr(II).[23]

Gansäuer and co-workers have also developed a similar system for epoxide ring-opening that uses catalytic Cp$_2$TiCl$_2$, Mn as the stoichiometric reductant, and [HCol]Cl (2,4,6-trimethylpyridine hydrochloride) in place of chlorosilanes to cleave the Ti−O bond.[24] This strategy was also extended to chromium-catalyzed NHK reactions, replacing Me$_3$SiCl with [HCol]Cl.[25] Kishi later reported the use of Cp$_2$ZrCl$_2$ as an effective transmetallating reagent for the chromium-catalyzed NHK reaction, providing increased substrate conversion compared to Me$_3$SiCl.[26]

Although the Cr(III) iodide CpCr[(XylNCMe)$_2$CH](I) was readily reduced to the Cr(II) compound **1** by commercial Mn powder (Scheme 3, path I),[8] the corresponding bromide and chloride complexes required the use of Mn activated with catalytic amounts of PbBr$_2$ or PbCl$_2$.[7] We now report that the Cr(III) hydroxide, **4**, and acetate analogue, CpCr[(XylNCMe)$_2$CH](O$_2$CMe), were also not reduced to compound **1** without the use of PbCl$_2$ activated Mn, while the alkoxide compound **7** did not react even with activated Mn at room temperature over a 24 h period.

Somewhat analogous to the system used by Gansäuer,[24] the $\mu$-oxo compound **3**, hydroxide **4**, and alkoxide **7** were all found to react with pyridinium halides to cleanly form the CpCr[(XylNCMe)$_2$CH](X) halides (Scheme 3, paths D, F,


dx.doi.org/10.1021/ic202233f | Inorg. Chem. 2012, 51, 688−700

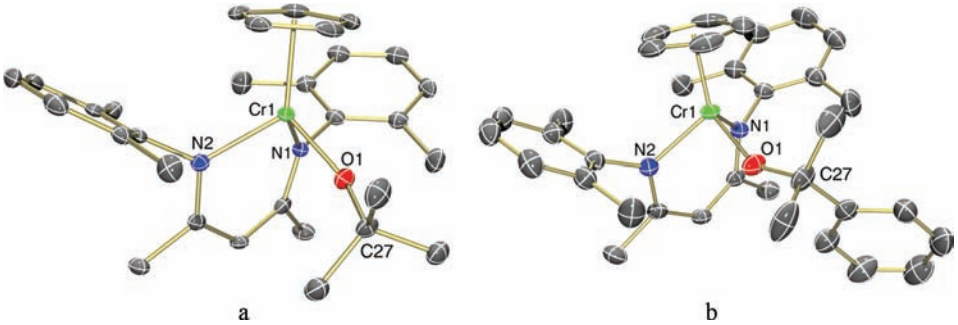


**Figure 3.** Thermal ellipsoid diagrams (50%) of (a) **6** and (b) **7**. All H atoms have been omitted for clarity.

and L, respectively), which, in turn, can be reduced to the Cr(II) compound **1** with activated Mn. Additionally, hydroxide **4** and alkoxide **7** both reacted with $PhCO_2H$ in a similar reaction to form the benzoate compound **5**.

The use of $Me_3SiCl$ to activate Mn powder was successful, providing an alternative to lead halide salts for the reduction of the Cr(III) bromide and chloride (**2**) complexes. The hydroxide compound **4** also reacted with $Me_3SiCl$ to break the Cr−O bond, giving the chloride compound **2** (Scheme 3, path F). Furthermore, the Cr(III) acetate compound CpCr-$[(XylNCMe)_2CH](O_2CMe)$ was readily converted to **2** by reaction with either $Me_3SiCl$ or $Cp_2ZrCl_2$, in the latter case generating a stoichiometric amount of $Cp_2Zr(Cl)(OAc)$ (Scheme 3, path G).

Interestingly, the alkoxide compound **7** was found to react with $Cp_2ZrCl_2$, as expected, to form compound **2** (Scheme 3, path L), but **7** was found to be completely unreactive toward $Me_3SiCl$ (2 days at room temperature) under anhydrous conditions. However, an identical reaction conducted with an additional 0.5 equiv of $H_2O$ led to conversion of alkoxide **7** to chloride **2** (UV−vis). It has been proposed by Wessjohann that Cr(III) alkoxides do not react directly with $Me_3SiCl$.[27] Additionally, Jacobsen reported that in the epoxide ring-opening reactions with $Me_3SiN_3$ catalyzed by Cr(III), the strict exclusion of water resulted in deactivation of the catalytic system while reactivation could be achieved with the addition of trace water, causing the formation of small amounts of $HN_3$.[28] It was therefore proposed that $HN_3$, and not $Me_3SiN_3$, was, in fact, the active species for the key Cr(III)−OR bond cleavage step. This mechanism is consistent with the observed reactivity of the Cr(III) alkoxide compound **7** with $Me_3SiCl$ in the presence of added water.

Treatment of the hydroxide compound **4**, the Cr(III) acetate compound $CpCr[(XylNCMe)_2CH](O_2CMe)$, and the Cr(III) enolate compound $CpCr[(XylNCMe)_2CH][OC(=CH_2)Ph]$ with in situ generated $MnI_2$ resulted in transmetalation to form the Cr(III) iodide complex (Scheme 3, paths F, G, and M, respectively),[29] which if conducted in the presence of excess Mn powder results in direct reduction to the Cr(II) compound **1**.[30] The $\mu$-oxo compound **3** was also found to react with $MnX_2$, where X = Cl or I, to form the appropriate Cr(III) halide species. Alternatively, the alkoxide compound **7** did not react with $MnI_2$ to form the Cr(III) iodide, potentially a contributing factor to the inability of activated Mn to reduce compound **7**.

**OAT Reactivity: $PPh_3$ Oxidation.** The $\mu$-oxo compound **3** rapidly reacted with $Ph_3PI_2$ causing a color change from orange to green (Scheme 5). The UV−vis spectrum of the reaction mixture was consistent with the formation of CpCr-

**Scheme 5**

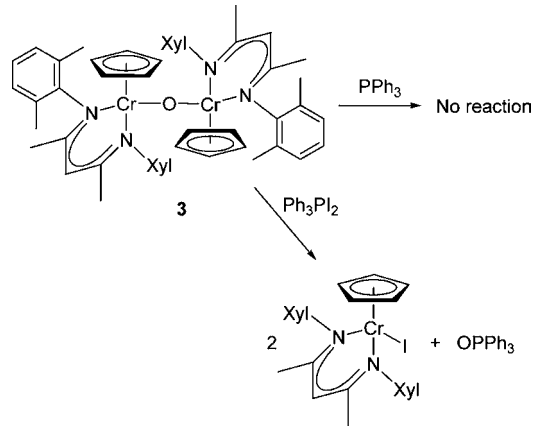


$[(XylNCMe)_2CH](I)$ and the $^{31}P$ NMR spectrum contained only one peak corresponding to $OPPh_3$.

The oxidation of $PPh_3$ was investigated to assess the stability of the cyclopentadienyl chromium $\beta$-diketiminate framework under catalytic oxidative conditions and to compare the reactivity of $\mu$-oxo **3** with other oxygen atom transfer (OAT) catalysts. Many of the examples of chromium catalyzed OAT involve a Cr(III)/Cr(V) redox couple where the Cr(III) must be sufficiently reducing to form a Cr(V) oxo, which then must be sufficiently oxidizing to react with organic substrates to achieve the oxo transfer.[31] The Cr corrole system of Gray and co-workers is an example of the Cr(III)/Cr(V) oxo redox couple; the Cr(V) oxo reacts quickly with $PPh_3$ to generate $OPPh_3$ but the Cr(III) is slow to react with $O_2$.[12h] This system also suffers from product inhibition where the reduced Cr(III) corrole coordinates $OPPh_3$, further reducing the rate of Cr(III) oxidation. Veige and co-workers adopted a tridentate pincer ligand that was found to increase the rate of Cr(III) oxidation by $O_2$, as a result of the open coordination site on the Cr center, created by moving from a tetra- to a tridentate ligand framework.[12k]

Alternatively, using a Cr(II)/Cr(IV) oxo redox couple presents two potential advantages: the increased reactivity of the reduced Cr(II) toward oxidation with $O_2$ and the expected higher reactivity of the Cr(IV) oxo species, compared to a Cr(V) analogue. The latter observation was reported for the Cr corrole system where single-electron reduction of the Cr(V) oxo compound of Gray and co-workers to an anionic Cr(IV) oxo species was proposed to result in both an increased electrophilicity and an increase in the unpaired electron density of the oxygen atom.[12j] Similarly, in situ generated aqueous


dx.doi.org/10.1021/ic202233f | Inorg. Chem. 2012, 51, 688−700

$CrO^{2+}$ reacted with $PPh_3$ to form $OPPh_3$ with a rate constant of $2.1(2) \times 10^3\ M^{-1}\ s^{-1}$.[32]

It was thought that a catalytic system could be achieved from a Cr(II) CpCr[$(ArNCMe)_2CH$] compound. As discussed above, the Cr(II) compound CpCr[$(XylNCMe)_2CH$], **1**, reacted rapidly with $O_2$ to form the bimetallic Cr(III) $\mu$-oxo compound **3**. Additionally, **1** does not readily coordinate $OPPh_3$ or other Lewis bases, avoiding the issue of product inhibition.[11f,12h] Unfortunately, the $\mu$-oxo compound **3** did not react with $PPh_3$, presumably as a result of the highly stable nature of the $\mu$-oxo core. The formation of **3** is thought to proceed through a terminal Cr(IV) oxo species: the monomeric CpCr[$(XylNCMe)_2CH$](O) oxo intermediate would be expected to be much more reactive toward OAT reactions.

By replacing the 2,6-dimethylphenyl groups of the $\beta$-diketiminate ligand with slightly larger 2,6-diethylphenyl the stability of the Cr(III) $\mu$-oxo species should be reduced due to the increased bulk being directed at the already strained Cr−O−Cr core, leading to an increased likelihood of a Cr(IV) oxo. The Cr(II) compound CpCr[$(DepNCMe)_2CH$], **1a**, was, in fact, found to catalyze the aerobic oxidation of $PPh_3$ to $OPPh_3$ (eq 2). Exposure of a solution of **1a** with a large excess of $PPh_3$

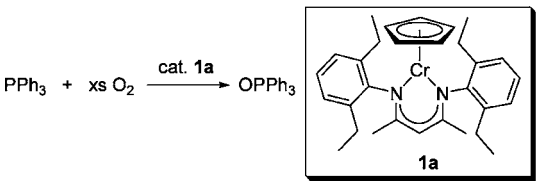


(2)

to one atmosphere of $O_2$ resulted in the formation of $OPPh_3$ with a maximum turnover number (TON; mol product/mol catalyst) of 20, based on isolated $OPPh_3$. Air was also found to be an effective source of oxygen for this reaction, as $^{31}P$ NMR analysis showed complete conversion of 6 equiv of $PPh_3$ upon air exposure over a period of approximately 10 min. TONs were ultimately limited under the reaction conditions as a result of catalyst deactivation.

**HAT Reactivity.** As discussed above, the $\mu$-oxo complex **3** did not react with excess pyridine *N*-oxide in THF. Alternatively, **3** was found to react with an excess of pyridine *N*-oxide in the presence of the hydrogen atom source $\gamma$-terpinene over a 2 day period at room temperature. Notably, complex **3** did not react with $\gamma$-terpinene in the absence of pyridine *N*-oxide, highlighting the need for an oxidant in the reaction. UV−vis analysis of the crude reaction mixture suggested that the product of the reaction was the Cr(III) hydroxide compound **4**. The solid-state molecular structure obtained from recrystallized **4** confirmed the intermolecular HAT, showing that the product of the reaction was the hydroxide complex **4** (Figure 4). The Cr−O bond length of 1.896(1) Å is slightly longer than the 1.814(2) Å reported for the cationic 5-coordinate Cr(III) hydroxide complex [$Tp^{tBu,Me}$Cr(OH)(pz′H)], prepared from the Cr(IV) oxo precursor undergoing a hydrogen atom abstraction from substrates containing C−H bond dissociation energies (BDEs) < 92 kcal/mol.[12g] Related hydrogen atom abstraction reactions of cyclohexadiene with well-defined Cr(V) oxo and Cr(III) superoxo complexes have been reported by Nam and co-workers.[13b,c]

A possible mechanism for the observed HAT reactivity is shown in Scheme 6. The lack of further oxidation of $\mu$-oxo **3** with excess pyridine *N*-oxide suggests that the reaction of

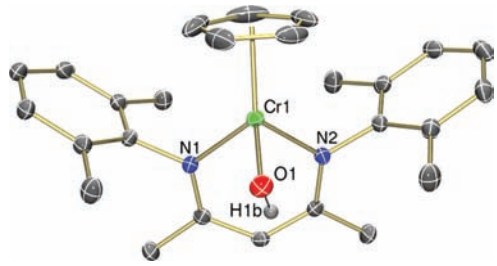


**Figure 4.** Thermal ellipsoid diagram (50%) of **4**. H atoms, with the exception of the hydroxide group, have been omitted for clarity. Disordered Cp and hydroxide ligands were each modeled in two orientations; in both cases, only one is shown.

Cr(II) complex **1** with pyridine *N*-oxide may be reversible. The steric demands of the 2,6-dimethylphenyl substituted $\beta$-diketiminate ligand apparently aid in the reversible dissociation of $\mu$-oxo **3**, analogous to the Cr porphyrin system described by Liston and West.[15] However, the proposed Cr(IV) oxo species generated is rapidly trapped by Cr(II) complex **1** in the absence of a substrate with weak C−H bonds. Similarly, the Cr(II) complex **1** does not react with $\gamma$-terpinene; so in the absence of oxidant, only a minute amount of Cr(III) hydroxide product **4** is presumably formed before the build up of complex **1** effectively precludes further consumption of $\mu$-oxo **3**. Significant conversion of $\mu$-oxo **3** to the HAT product Cr(II) hydroxide **4** is only achieved when both $\gamma$-terpinene and pyridine *N*-oxide are present. No further reaction of compound **4** was observed with the excess $\gamma$-terpinene.

The HAT reactivity ascribed to the putative chromium oxo species in Scheme 6 is consistent with the expected strength of the O−H bond in **4**, the Cr(III) hydroxide product.[33] This rationale has been used to explain the radical reactivity of aqueous $CrO^{2+}$,[34] as well as biologically relevant Cr(IV) and Cr(V) complexes.[35] Work with iron imido complexes have examined the role of N-based radical character on HAT reactivity.[36] We were therefore interested in isolating an analogue of the monomeric oxo intermediate in Scheme 6 to evaluate the degree of oxo-based radical character[37] and its possible impact on reactivity.[38]

Reaction of the bulkier 2,6-diethylphenyl Cr(II) compound **1a** with pyridine *N*-oxide or $O_2$ resulted in a rapid color change to orange, consistent with Cr(III) $\mu$-oxo formation, followed by a further color change to green. The decrease in stability of the Cr(III) $\mu$-oxo with increased steric bulk of the $\beta$-diketiminate ligand is consistent with the observed $PPh_3$ oxidation reactivity, suggesting a Cr(IV) oxo intermediate is the active OAT species in solution. The UV−vis spectrum of the green crude reaction mixture was consistent with the formation of a Cr(III) hydroxide compound, but no tractable products could be isolated from the reactions in a variety of different solvents. Addition of the hydrogen atom source $\gamma$-terpinene to the reaction of the Cr(II) compound **1a** with pyridine *N*-oxide, analogous to the reaction of **1** to form hydroxide **4**, cleanly provided the Cr(III) hydroxide compound CpCr-[$(DepNCMe)_2CH$](OH), **4a** (Scheme 7). Compound **4a** was more readily prepared compared to **4**, giving a higher yield with reduced reaction time, also consistent with the decreased stability of the bimetallic Cr(III) $\mu$-oxo species when the larger $\beta$-diketiminate ligand framework is present.

The formation of Cr(III) hydroxide species in the absence of $\gamma$-terpinene suggested that intermolecular HAT from solvent or even intramolecular HAT from the ligands was the route to the


dx.doi.org/10.1021/ic202233f | Inorg. Chem. 2012, 51, 688−700

Scheme 6

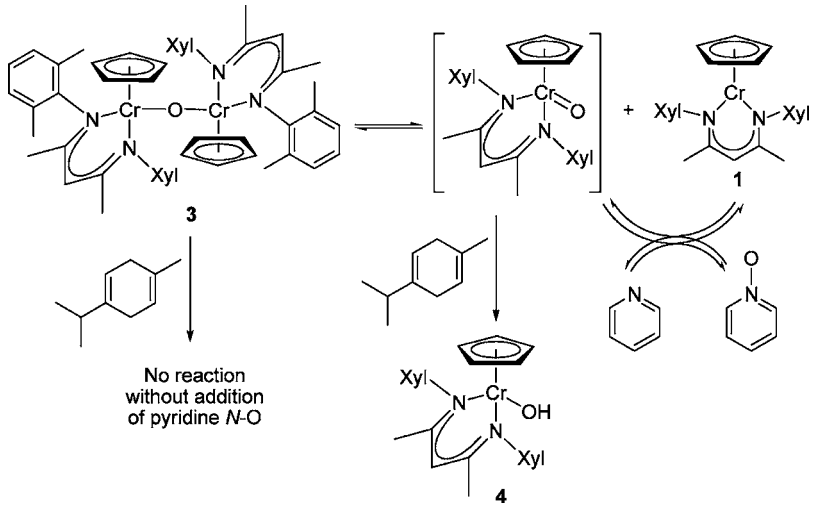


Scheme 7

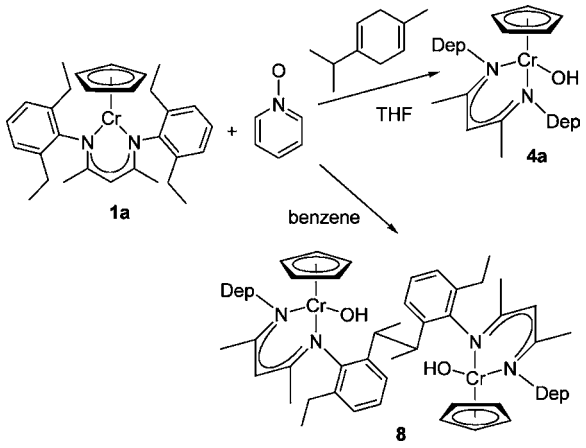


Cr(III) hydroxide formation. Compound **1a** was reacted with pyridine *N*-oxide in benzene to remove the possibility of solvent based HAT (Scheme 7). The isolated product was characterized by X-ray crystallography as a Cr(III) hydroxide dimer, compound **8** (Figure 5). Compound **8** has similar bond lengths to the monometallic Cr(III) hydroxide **4** with Cr−O bond lengths of 1.8569(13) Å and 1.8654(13) Å and Cr−N bond lengths in the range of 2.0132(14)−2.0282(13) Å.

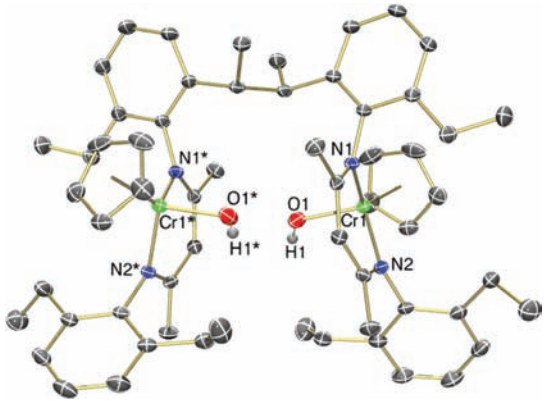


**Figure 5.** Thermal ellipsoid diagram (50%) of **8**. H atoms, with the exception of the hydroxide groups, have been omitted for clarity. Compound **8** crystallizes with two independent molecules in the asymmetric unit, each residing on a 2-fold axis of rotation.

In the absence of external hydrogen atom sources, the Cr(IV) oxo intermediate underwent intramolecular HAT from the secondary benzylic groups of the $\beta$-diketiminate ligand followed by intermolecular radical C−C bond formation to generate the Cr(III) hydroxide dimer **8**. Examples of ligand based C−H activation of diiminepyridine backbone methyl groups resulting in intermolecular C−C coupling have been previously reported.[39] An example of intramolecular HAT from a $\beta$-diketiminate ligand was reported by Holland and co-workers with an imido Fe(III) compound that results in *intra*molecular C−C bond formation.[36b]

**Synthesis of {CpCr[(HIPTNCMe)$_2$CH]}$_2$($\mu$-O).** Replacing the ortho substituents on the N-aryl groups of the $\beta$-diketiminate ligand with meta substituents removes the reactive benzylic C−H bonds in proximity to the Cr−O reactive site. The size of bulky substituents must be substantially increased when placed in meta positions if bimetallic $\mu$-oxo formation is to be discouraged. Piers used the hexaisopropylterphenyl {HIPT, [3,5-(2,4,6-$^i$Pr$_3$C$_6$H$_2$)$_2$C$_6$H$_3$]} substituents pioneered by Schrock[40] to prevent unwanted C−H activation of the $\beta$-diketiminate ligand.[41]

Preparation of the Cr(II) compound CpCr[(HIPTNCMe)$_2$CH] was achieved by the standard method of reacting $CrCl_2$ with 1 equiv of NaCp followed by 1 equiv of the deprotonated $\beta$-diketiminate ligand to form a solution that was green to incident and magenta to transmitted light, similar to that of the Cr(II) compound **1**. The high solubility of the complex in hexanes precluded isolation by recrystallization. The CpCr[(HIPTNCMe)$_2$CH] compound reacted with pyridine *N*-oxide to form an orange solution with an absorption in the UV−vis spectrum at 371 nm and a shoulder at 475 nm, analogous to the $\mu$-oxo compound **3** (Scheme 8). The solid-state molecular structure obtained from the isolated orange crystalline material exhibited extensive disorder and low data quality, as has previously been observed in metal complexes bearing ligands with HIPT substituents.[40c,d] The complex also crystallized with unresolvable residual electron density, likely from disordered solvent in the lattice. Due to these difficulties, the full composition of compound **9** is unknown, and the specific bond lengths and angles for **9** may be somewhat unreliable. However, the structure confirmed that despite the


dx.doi.org/10.1021/ic202233f | *Inorg. Chem.* 2012, 51, 688−700

**Scheme 8**

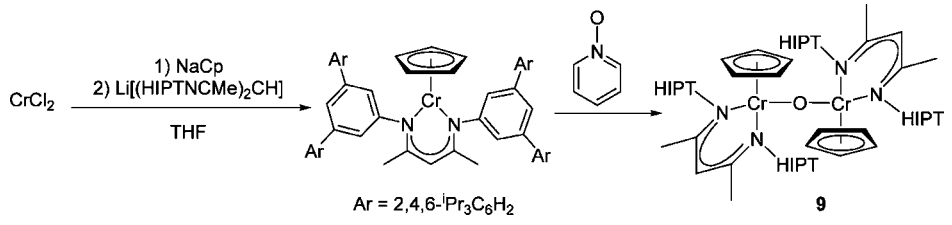


introduction of large meta substituents, **9** has a bimetallic Cr(III) $\mu$-oxo core (Figure 6).

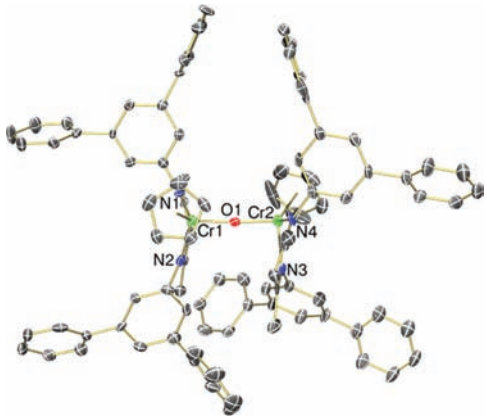


**Figure 6.** Thermal ellipsoid diagram (50%) of **9**. All H atoms and isopropyl groups have been omitted for clarity.

Compound **9** exhibits a Cr−O−Cr angle (174.3(2)°) that is essentially identical to the $\mu$-oxo compound **3** (174.5(2)°). The Cr−O bond lengths (1.784(4) and 1.786(3) Å), in contrast, are significantly shorter compared to **3** (1.834(3) Å). Additionally, reactivity studies of {CpCr[(HIPTNCMe)$_2$CH]}$_2$($\mu$-O), **9**, suggested that the compound was actually less reactive than compound **3**. Unlike **3**, compound **9** did not react with $H_2O$ nor was there any reaction with excess pyridine *N*-oxide and $\gamma$-terpinene upon stirring for 10 days. The lack of protonolysis and HAT reactivity in combination with the shorter Cr−O bond lengths indicated that there was no significant increase in steric strain of the bimetallic $\mu$-oxo species between the HIPT and Xylyl derivatives of the $\beta$-diketiminate ligand.

**Catalytic HAT.** Attempts to render a catalytic HAT reaction based on a Cr(IV) oxo catalyst with $O_2$ as the oxidant, founded on the stoichiometric reactivity discussed above, proved challenging. When Mn was used as the stoichiometric reductant the catalyst turnovers were ultimately limited by one of two factors: either the Mn was deactivated by the presence of the oxidant and would no longer reduce the Cr(III) intermediates, as was the case with $PbCl_2$ activated Mn, or the oxidant was rapidly consumed by the activated Mn to form Mn oxides, as was the case with $I_2$ or $Me_3SiCl$ activating agents.[42] The best result for the catalytic in Cr conversion of $\gamma$-terpinene to *p*-cymene was limited to 4 turnovers of the catalyst (2 equiv of *p*-cymene per Cr). The optimal reaction conditions were found with a catalytic amount of CpCr[(DepNCMe)$_2$CH](Cl), **2a**, excess Zn as the stoichiometric reductant, and either $Me_3SiCl$ or $PbCl_2$ as the activating agent for the Zn. A discussion of the attempted HAT reactivity is presented in the Supporting Information.

**Haloacetal Cyclization.** We reported a chromium-catalyzed radical cyclization of bromo and chloro acetals. Cyclization of the bromo substrates was achieved in high yields with only 2 mol % Cr catalyst loadings (Table 2, entry 1).[7] The active catalyst species in the reaction, compound **1**, is extremely air-sensitive, forming the Cr(III) $\mu$-oxo compound **3** in the presence of oxygen. As a result, the halo acetal reactions must be performed with the strict exclusion of oxygen. We now report the use of $\mu$-oxo compound **3** as a catalyst precursor and present conditions that allow for compound **3** to be converted back to the active catalyst under catalytically relevant reaction conditions.

**Table 2. Chromium-Catalyzed Bromoacetal Radical Cyclization**[a]

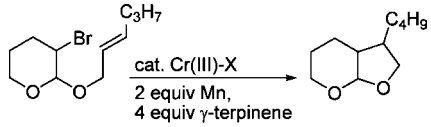


| entry | Cr Catalyst | additives | yield[b] |
|---|---|---|---|
| 1 | 2 mol % Cr(III)-Br | <1 mol % $PbBr_2$ | 93% (82/18) |
| 2 | 1 mol % **3** | 1 mol % $PbBr_2$ | <40% |
| 3 | 1 mol % **3** | 3 mol % [HLut]Br | 83% (82/18)[c] |
| 4 | 1 mol % **3** | 3 mol % [HLut]Br, 1 mol % $PbBr_2$ | 90% (82/18) |
| 5 | 2 mol % Cr(III)-Br | 10 mol % $Me_3SiCl$ | 87% (82/18)[d] |
| 6 | 2 mol % Cr(III)-Br | 10 mol % $Me_3SiCl$ | 92% (80/20)[e] |

[a]Reaction conditions: substrate (1 mmol), Mn (2 equiv), $\gamma$-terpinene (4 equiv), THF (4 mL), 38.5 h at 50 °C. [b]Isolated yields. Diastereomeric ratios are in parentheses. [c]Compound **3** mixed with 3 mol % [HLut]Br and Mn (2 equiv) for 4 h prior to addition of substrate. No reaction is observed without premixing step. [d]24 h reaction time. [e]Reagents were mixed under air prior to reaction for 22 h at 65 °C.

In a control experiment, the direct use of compound **3** as catalyst precursor under the standard reaction conditions led to <40% conversion (entry 2), and no substrate conversion was observed with 1 mol % of **3** if the $PbBr_2$ additive was replaced with 3 mol % of lutidinium bromide. However, the $\mu$-oxo compound **3** was readily reduced to **1** if 2 equiv of [HLut]Br and an excess of Mn were added before the haloacetal and $\gamma$-terpinene (Scheme 3, paths D and I). Subsequent addition of the desired bromo substrate under standard reaction conditions resulted in an 83% isolated yield (Table 2, entry 3), only a 10% decrease in yield compared to the standard conditions using the CrCr[(XylNCMe)$_2$CH](Br) catalyst. Entry 4 shows the optimized reaction conditions with only 1 mol % of the $\mu$-oxo **3** providing 90% isolated yield of the desired cyclized product.

It was also determined that a substoichiometric amount of $Me_3SiCl$ could be used to activate the Mn in place of the $PbBr_2$


dx.doi.org/10.1021/ic202233f | Inorg. Chem. 2012, 51, 688−700

Table 3. X-ray Crystallographic Data for Compounds 3, 4, 5, and 5a

| | $3\cdot{}^1/_2C_6H_{14}$ | 4 | 5 | 5a |
|---|---|---|---|---|
| formula | $C_{55}H_{67}N_2Cr_2O$ | $C_{26}H_{31}N_2OCr$ | $C_{33}H_{35}N_2O_2Cr$ | $C_{41}H_{51}N_2O_2Cr$ |
| formula weight | 904.13 | 439.53 | 543.63 | 655.84 |
| crystal color, habit | black, needle | black, prism | black-green, prism | dark green, plate |
| crystal dimensions, mm | 0.03 × 0.15 × 0.15 | 0.20 × 0.30 × 0.35 | 0.25 × 0.30 × 0.50 | 0.25 × 0.35 × 0.50 |
| crystal system | triclinic | monoclinic | triclinic | monoclinic |
| space group | $P\bar{1}$ | $P\ 2_1/n$ | $P\bar{1}$ | $P\ 2_1/c$ |
| $a$, Å | 9.1063(8) | 12.0157(3) | 9.5648(10) | 17.658(2) |
| $b$, Å | 14.7309(14) | 15.0102(4) | 12.8067(15) | 10.735(2) |
| $c$, Å | 18.546(2) | 13.2704(3) | 13.3869(16) | 19.833(4) |
| $\alpha$, deg | 90.341(3) | 90 | 63.185(6) | 90 |
| $\beta$, deg | 95.604(4) | 109.716(1) | 73.615(6) | 91.067(7) |
| $\gamma$, deg | 107.903(4) | 90 | 82.412(6) | 90 |
| $V$, Å$^3$ | 2354.4(4) | 2253.1(1) | 1404.0(3) | 3768(1) |
| $Z$ | 2 | 4 | 2 | 4 |
| $D_{calc}$, g/cm$^3$ | 1.275 | 1.296 | 1.286 | 1.156 |
| $F_{000}$ | 960 | 932 | 574 | 1404 |
| $\mu$(Mo K$\alpha$), cm$^{-1}$ | 5.05 | 5.27 | 4.40 | 3.38 |
| data images (no., $t/s$) | 832, 25 | 1067, 10 | 2344, 5 | 3106, 5 |
| $2\theta_{max}$ | 45.0° | 60.1° | 56.2° | 56.0° |
| reflcns measrd | 16713 | 25873 | 29288 | 172767 |
| unique reflcn, $R_{int}$ | 5987, 0.083 | 6591, 0.027 | 6734, 0.029 | 16687, 0.082 |
| absorption, $T_{min}$, $T_{max}$ | 0.643, 0.985 | 0.821, 0.900 | 0.704, 0.896 | 0.671, 0.919 |
| obsrvd data ($I > 2.00\sigma(I)$) | 3478 | 5605 | 5627 | 8110 |
| no. parameters | 572 | 357 | 349 | 426 |
| R1, wR2 ($F^2$, all data) | 0.127, 0.113 | 0.043, 0.100 | 0.048, 0.102 | 0.096, 0.135 |
| R1, wR2 ($F$, $I > 2.00\sigma(I)$) | 0.052, 0.089 | 0.034, 0.094 | 0.038, 0.096 | 0.049, 0.124 |
| goodness of fit | 0.99 | 1.04 | 1.04 | 1.01 |
| max, min peak, e$^-$/Å$^3$ | 0.34, −0.42 | 0.47, −0.33 | 0.35, −0.41 | 0.40, −0.58 |

under the standard reaction conditions, with only a slight decrease in yield (entry 5). Most notable is the result in entry 6, where the reaction vessel was charged with the reagents and solvent under ambient atmosphere, after which the headspace of the reaction vessel was purged with $N_2$ before being sealed. The reaction was heated to 65 °C for 22 h to afford a 92% isolated yield upon workup.

The success of the reaction can be attributed to the fact that $Me_3SiCl$ activated Mn reacts rapidly with $O_2$ to form Mn oxides, the same reason the Mn was not effective for the HAT reactions. The activated Mn scrubbed the reaction of trace oxygen before the Cr(III) bromide catalyst was reduced to the air-sensitive Cr(II) state, thereby alleviating the need to meticulously exclude trace oxygen from the haloacetal cyclization reactions.

## CONCLUSIONS

Although potent single-electron reductants such as Cr(II), Sm(II),[9] and Ti(III)[10] are used for the stoichiometric generation of carbon-based radicals, several challenges must be overcome before these highly air-sensitive reagents can be employed catalytically. The strong metal−oxygen bonds in the products must be broken, and a sufficiently powerful stoichiometric reductant is required to reform the active low-valence species. Fürstner's $Me_3SiCl$/Mn multicomponent system made ancillary ligand development feasible for asymmetric NHK reactions catalytic in chromium.[21] While high-spin monomeric Cr(II) compounds are intrinsically air-sensitive, understanding how reactive species can be regenerated from air-oxidized complexes under catalytically relevant conditions is expected to make Cr-based catalysts more widely applicable.[22,43]

Despite their complexity, multicomponent catalytic systems are remarkably amenable to mechanistic interrogation, as each individual step can be investigated separately. The study of the paramagnetic Cr(III) compounds described in this paper was assisted by the crystallinity imparted by the cyclopentadienyl and $\beta$-diketiminate ancillary ligands, and by the distinctive color changes that accompany the variation of the X group in the Cr(III) CpCr[(ArNCMe)$_2$CH](X) complexes. The $\mu$-oxo dimer was readily converted to Cr(III)−X species using reagents with known compatibility with Mn as a stoichiometric reductant. Replacing $PbBr_2$ with 10 mol % $Me_3SiCl$ allowed the previously reported Cr-catalyzed radical cyclization of a bromoacetal to be set up under ambient conditions. The CpCr[(ArNCMe)$_2$CH] framework proved to be remarkably robust with respect to air oxidation, protonolysis, salt-metathesis, transmetalation, and reduction reactions.

In the presence of pyridine $N$-oxide, the $\mu$-oxo dimer underwent an intermolecular HAT reaction with $\gamma$-terpinene. This reactivity was ascribed to a putative monomeric oxo intermediate and is consistent with both the expected strength of the O−H bond of the Cr(III) hydroxide product and with possible oxo-based radical character. The use of very large HIPT substituents on the $\beta$-diketiminate ancillary ligand did not prevent $\mu$-oxo dimer formation. However, changing the N-aryl ortho substituents from methyl to ethyl did permit the Cr-catalyzed aerobic oxidation of $PPh_3$. In the absence of OAT or HAT substrates, a product consistent with intramolecular ligand HAT followed by radical C−C bond formation was structurally characterized.


dx.doi.org/10.1021/ic202233f | Inorg. Chem. 2012, 51, 688−700

Table 4. X-ray Crystallographic Data for Compounds 6, 7, 8, and 9

| | 6 | 7 | 8 | 9 |
|---|---|---|---|---|
| formula | $C_{30}H_{39}N_2OCr$ | $C_{35}H_{41}N_2OCr$ | $C_{60}H_{76}N_4O_2Cr_2$ | $C_{164}H_{220}N_4OCr_2$ |
| formula weight | 495.63 | 439.53 | 989.25 | 2367.44 |
| crystal color, habit | black, prism | Black-green, plate | black, prism | orange, prism |
| crystal dimensions, mm | 0.135 × 0.15 × 0.16 | 0.03 × 0.50 × 0.50 | 0.10 × 0.17 × 0.25 | 0.125 × 0.16 × 0.22 |
| crystal system | monoclinic | monoclinic | monoclinic | monoclinic |
| space group | $P2_1/n$ | $P2_1/n$ | $P2/c$ | $P2_1/c$ |
| $a$, Å | 16.302(3) | 11.5614(10) | 16.0439(8) | 31.054(3) |
| $b$, Å | 9.0161(16) | 8.9497(8) | 11.9799(5) | 18.839(2) |
| $c$, Å | 18.449(3) | 29.309(3) | 27.4399(13) | 31.163(3) |
| $\alpha$, deg | 90 | 90 | 90 | 90 |
| $\beta$, deg | 99.280(4) | 99.964(5) | 103.200(2) | 111.582(2) |
| $\gamma$, deg | 90 | 90 | 90 | 90 |
| $V$, Å$^3$ | 2676.2(8) | 2986.9(5) | 5134.7(6) | 16953(3) |
| $Z$ | 4 | 4 | 4 | 4 |
| $D_{calc}$, g/cm$^3$ | 1.230 | 1.240 | 1.280 | 0.928 |
| $F_{000}$ | 1060 | 1188 | 2112 | 5152 |
| $\mu$(Mo K$\alpha$), cm$^{-1}$ | 4.52 | 4.12 | 4.71 | 1.72 |
| data images (no., $t$/$s$) | 967, 60 | 1173, 10 | 1177, 10 | 824, 90 |
| $2\theta_{max}$ | 48.3° | 56.0° | 60.1° | 45.1° |
| reflcns measrd | 15747 | 32185 | 58708 | 83553 |
| unique reflcn, $R_{int}$ | 4261, 0.041 | 7184, 0.037 | 15030, 0.046 | 21958, 0.127 |
| absorption, $T_{min}$, $T_{max}$ | 0.866, 0.941 | 0.856, 0.988 | 0.895, 0.954 | 0.738, 0.979 |
| obsrvd data ($I > 2.00\sigma(I)$) | 3313 | 5348 | 10647 | 12172 |
| no. parameters | 312 | 360 | 617 | 1592 |
| R1, wR2 ($F^2$, all data) | 0.066, 0.112 | 0.067, 0.112 | 0.076, 0.122 | 0.145, 0.231 |
| R1, wR2 ($F$, $I > 2.00\sigma(I)$) | 0.044, 0.102 | 0.042, 0.101 | 0.046, 0.108 | 0.085, 0.204 |
| goodness of fit | 1.06 | 1.03 | 1.02 | 0.949 |
| max, min peak, e$^-$/Å$^3$ | 0.34, −0.35 | 0.31, −0.36 | 0.50, −0.35 | 0.63, −0.56 |

## EXPERIMENTAL SECTION

**General Considerations.** Unless otherwise indicated, all reactions were carried out under nitrogen using standard Schlenk and glovebox techniques. Hexanes, diethylether, $CH_2Cl_2$, and THF were purified by passage through activated alumina and deoxygenizer columns from Glass Contour Co. (Laguna Beach, CA). Celite (Aldrich) was dried overnight at 120 °C before being evacuated and then stored under nitrogen. γ-Terpinene was degassed by three freeze−vacuum−thaw cycles and stored under nitrogen prior to use. $C_6D_6$ was dried over sodium/benzophenone, purified by vacuum distillation, degassed by three freeze−vacuum−thaw cycles, and stored under nitrogen. $CDCl_3$ was used as received.

Pyridine *N*-oxide, benzoic acid, $AgO_2CPh$, and KO$^t$Bu were used as received. $KOC(Me)_2Ph$ was prepared by reacting $HOC(Me)_2Ph$ with 1 equiv of $KN(SiMe_3)_2$ in 10 mL of hexanes/toluene (5:1), while stirring for 2 h. The product was isolated by vacuum filtration, rinsed with hexanes, dried under vacuum, and stored under $N_2$. CpCr[(XylNCMe)$_2$CH], (**1**),[44] CpCr[(DepNCMe)$_2$CH], (**1a**),[17] CpCr[(DppNCMe)$_2$CH], (**1b**),[45] CpCr[(XylNCMe)$_2$CH](Cl), (**2**),[17] and $Ph_3PI_2$[46] were prepared according to the literature procedures. H[(HIPTNCMe)$_2$CH] was prepared with a slight modification to the literature procedure.[41]

$^1$H and $^{31}$P spectra were recorded on a Varian Mercury Plus 400 spectrometer. UV−visible spectroscopic data was collected on Varian Cary 100 Bio or Shimadzu UV-2550 UV−visible spectrophotometers in a specially constructed cell for air-sensitive samples: a Kontes Hi-Vac Valve with PTFE plug was attached by a professional glassblower to a Hellma 10 mm path length quartz absorption cell with a quartz-to-glass graded seal. Elemental analyses were performed by Guelph Chemical Laboratories, Guelph, ON, Canada or by the UBC Department of Chemistry microanalytical services. Solution magnetic susceptibilities were determined by the Evans method.[47]

**X-ray Crystallography.** All crystals were mounted on a glass fiber, and measurements were made on a Bruker X8 APEX II diffractometer with graphite-monochromated Mo K$\alpha$ radiation. The data were collected at a temperature of −100 ± 1 °C in a series of $\phi$ and $\omega$ scans in 0.50° oscillations. Data were collected and integrated using the Bruker SAINT software package[48] and were corrected for absorption effects using the multiscan technique (SADABS).[49] The data were corrected for Lorentz and polarization effects. All structures were solved by direct methods.[50] All non-hydrogen atoms were refined anisotropically (unless otherwise mentioned below). All hydrogen atoms were placed in calculated positions but not refined. All refinements were performed using the SHELXTL crystallographic software package of Bruker-AXS.[51] The molecular drawings were generated by the use of ORTEP-3[52] and POV-Ray. X-ray crystallographic data for compounds **3**, **4**, **5**, and **5a** are shown in Table 3. X-ray crystallographic data for compounds **6**, **7**, **8**, and **9** are shown in Table 4.

Compound **3** crystallizes with one-half-molecule of hexanes (residing on an inversion center) in the asymmetric unit. Both the cyclopentadienyl ligand and the hydroxide ligand of compound **4** were disordered: each was subsequently modeled in two orientations. Compound **8** crystallizes with two independent molecules in the asymmetric unit, each residing on a 2-fold axis of rotation.

Compound **5** crystallizes as a two-component twin, with the second component related to the first by a rotation of 180° about the axis perpendicular to the (001) plane. The data was integrated for both components, including both overlapping and non-overlapping data. Subsequent refinements were carried out using the HKLF 5 format data set containing all reflections from both twin components. The fraction of the second twin component refined to a value of 0.406(1).

Compound **9** crystallizes with unresolvable residual electron density, likely from disordered solvent, in the lattice. The structure was refined without modeling any solvent molecules, then the PLATON/SQUEEZE[53] program was employed to search the cell for solvent accessible voids, and then to correct the X-ray diffraction data to eliminate any residual electron density found in those voids. The result from this procedure removed 840 residual electron density


dx.doi.org/10.1021/ic202233f | Inorg. Chem. 2012, 51, 688−700

from the unit cell, or approximately 210 electrons per asymmetric unit. Because it is not possible to properly identify the solvent, the values for the formula weight, etc., reflect only those atoms found in the atom list.

**Preparation of {CpCr[(XylNCMe)$_2$CH]}$_2$($\mu$-O) (3).** CpCr[(XylNCMe)$_2$CH] (**1**) (495 mg, 1.17 mmol) was placed in a round-bottom flask followed by the addition of 61.8 mg (0.65 mmol, 0.55 equiv) of pyridine *N*-oxide and approximately 10 mL of hexanes. After stirring overnight, the orange precipitate was isolated, rinsed with a small amount of diethyl ether, and dried to produce an orange powder (408 mg, 81%). $\mu_{eff}$ (Evans, $CDCl_3$) = 2.39 $\mu_\beta$. Anal. calcd. for $C_{52}H_{60}N_2Cr_2O$: C, 72.53; H, 7.02; N, 6.51. Found: C, 72.87; H, 6.87; N, 6.96. UV−vis (hexanes; $\lambda_{max}$, nm ($\varepsilon$, $M^{-1}$ $cm^{-1}$)): 362 (20700), 471 (sh).

**Preparation of CpCr[(XylNCMe)$_2$CH](OH) (4).** Compound **1** (100 mg, 0.237 mmol) was placed in a Schlenk flask followed by the addition of THF, 200 $\mu$L (1.25 mmol, 5.25 equiv) of $\gamma$-terpinene, and 110 mg (1.16 mmol, 4.89 equiv) of pyridine *N*-oxide. The solution quickly turned orange, and upon stirring for 2 days, it turned green, at which point the volatiles were removed *in vacuo*. The residue was extracted with hexanes, filtered over Celite, and the solvent was again removed *in vacuo*. The residue was extracted with a minimum amount of hexanes (3 mL), filtered, and cooled to −35 °C to provide black crystals of **4** (36 mg, 35%) in three crops. Anal. calcd. for $C_{26}H_{31}N_2CrO$: C, 71.05; H, 7.11; N, 6.37. Found: C, 70.94; H, 7.11; N, 6.50. UV−vis (hexanes; $\lambda_{max}$, nm ($\varepsilon$, $M^{-1}$ $cm^{-1}$)): 387 (9280), 503 (730), 614 (730).

**Preparation of CpCr[(DepNCMe)$_2$CH](OH) (4a).** Compound **4a** was prepared in a similar manner to compound **4** with CpCr[(DepNCMe)$_2$CH] (**1a**) (94.1 mg, 0.197 mmol), $\gamma$-terpinene (300 $\mu$L, 1.86 mmol, 9.44 equiv), and pyridine *N*-oxide (36.9 mg, 0.388 mmol, 1.97 equiv). The reaction mixture was stirred overnight. Workup and cooling to −35 °C in hexanes (2 mL) provided 57.3 mg (59%) of **4a**. Anal. calcd. for $C_{30}H_{39}N_2CrO$: C, 72.70; H, 7.93; N, 5.65. Found: C, 71.18; H, 7.99; N, 5.64. UV−vis (hexanes; $\lambda_{max}$, nm ($\varepsilon$, $M^{-1}$ $cm^{-1}$)): 388 (10400), 503 (740), 614 (760).

**Preparation of CpCr[(XylNCMe)$_2$CH](O$_2$CPh) (5).** *Method A.* Compound **2** (49.3 mg, 0.108 mmol) and $AgO_2CPh$ (24.4 mg, 0.107 mmol, 1.0 equiv) were placed in a Schlenk flask, followed by the addition of $CH_2Cl_2$ (20 mL). After stirring overnight, the volatiles were removed *in vacuo*; the residue was extracted with $Et_2O$ (25 mL) and filtered under ambient atmosphere. The volatiles were again removed *in vacuo*; the residue was extracted with approximately 15 mL of hexanes/$Et_2O$ (3:2) and concentrated, and the resulting green solution was cooled to −20 °C to provide black crystals of **5** (34.5 mg, 60%) in two crops. Anal. calcd. for $C_{33}H_{35}N_2O_2Cr$: C, 72.91; H, 6.49; N, 5.15. Found: C, 73.02; H, 6.33; N, 5.18. UV−vis (hexanes; $\lambda_{max}$, nm ($\varepsilon$, $M^{-1}$ $cm^{-1}$)): 413 (9320), 503 (680), 584 (770).

*Method B.* Compound **3** (119.5 mg, 0.139 mmol) and benzoic acid (34.4 mg, 0.282 mmol, 2.03 equiv) were placed in a Schlenk flask, followed by the addition of THF (30 mL). The solution changed color from orange to green and was stirred for 3 days; at which point, the volatiles were removed *in vacuo*, and the residue was extracted with approximately 5 mL of hexanes and 2 mL of $CH_2Cl_2$, concentrated, and cooled to −20 °C to provide **5** (98.7 mg, 66%) in two crops with an identical UV−visible spectrum to the product obtained from method A.

**Preparation of CpCr[(DppNCMe)$_2$CH](O$_2$CPh) (5b).** Compound **1b** (198 mg, 0.370 mmol) and $AgO_2CPh$ (85.7 mg, 0.374 mmol, 1.01 equiv) were placed in a Schlenk flask followed by the addition of THF (15 mL). After stirring overnight, the volatiles were removed *in vacuo*; the residue was extracted with hexanes and filtered over Celite. The green solution was concentrated to a volume of approximately 2 mL and cooled to −35 °C to provide black crystals of **5b** (106 mg, 43%). Anal. calcd. for $C_{35}H_{41}N_2CrO$: C, 75.08; H, 7.84; N, 4.27. Found: C, 74.98; H, 7.95; N, 4.21. UV−vis (hexanes; $\lambda_{max}$, nm ($\varepsilon$, $M^{-1}$ $cm^{-1}$)): 416 (10200), 584 (830).

**Preparation of CpCr[(XylNCMe)$_2$CH][OC(Me)$_3$] (6).** Compound **2** (53.2 mg, 0.116 mmol) was placed in a Schlenk flask, followed by the addition of $Et_2O$ (7 mL), and KO$^t$Bu (15.2 mg, 0.135 mmol, 1.17 equiv) suspended in $Et_2O$ (3 mL). After stirring for 4 days, the volatiles were removed *in vacuo*; the residue was extracted with hexanes and filtered over Celite. The solution was concentrated to a volume of approximately 0.5 mL and cooled to −35 °C to provide black crystals of **6** (24.0 mg, 42%) in two crops. Anal. calcd. for $C_{30}H_{39}N_2CrO$: C, 72.70; H, 7.93; N, 5.65. Found: C, 71.16; H, 7.93; N, 5.58. UV−vis (hexanes; $\lambda_{max}$, nm ($\varepsilon$, $M^{-1}$ $cm^{-1}$)): 393 (8620), 492 (880), 725 (550).

**Preparation of CpCr[(XylNCMe)$_2$CH][OC(Me)$_2$Ph] (7).** Compound **2** (59.8 mg, 0.131 mmol) was placed in a Schlenk flask followed by the addition of THF (7 mL). The addition of a 2 mL THF solution of KOC(Me)$_2$Ph (23.2 mg, 0.133 mmol, 1.02 equiv) caused a rapid color change from green to green−orange. After stirring for 5 days, the volatiles were removed *in vacuo*; the residue was extracted with hexanes and filtered over Celite. The solution was concentrated to a volume of approximately 0.5 mL and cooled to −35 °C to provide black crystals of **7** (50.7 mg, 70%). Anal. calcd. for $C_{35}H_{41}N_2CrO$: C, 75.38; H, 7.41; N, 5.02. Found: C, 73.81; H, 7.46; N, 5.04. UV−vis (hexanes; $\lambda_{max}$, nm ($\varepsilon$, $M^{-1}$ $cm^{-1}$)): 395 (8920), 491 (640), 740 (450).

**Preparation of {CpCr[(DepNCMe)$_2$CH](OH)}$_2$ (8).** CpCr[(DepNCMe)$_2$CH] (**1a**) (50.2 mg, 0.105 mmol) and pyridine *N*-oxide (10.7 mg, 0.113 mmol, 1.1 equiv) were placed in a round-bottom flask, followed by the addition of benzene (5 mL). The reaction mixture was stirred at room temperature overnight, followed by removal of the solvent *in vacuo*. The residue was extracted with hexanes (1 mL), filtered over Celite, and cooled to −35 °C to provide a black microcrystalline solid (17.7 mg) in two crops. A third crop of crystals (4.4 mg, 8%) suitable for X-ray crystallography was isolated and identified as compound **8**. The UV−visible spectrum of **8** was essentially indistinguishable from the corresponding monomeric Cr(III) hydroxide complex **4a**: UV−vis (hexanes; $\lambda_{max}$, nm): 388, 503, 614.

**Preparation of {CpCr[(HIPTNCMe)$_2$CH]}$_2$($\mu$-O) (9).** H[(HIPTNCMe)$_2$CH] (136 mg, 0.129 mmol, 1.06 equiv) was placed in a Schlenk flask, dissolved in THF (5 mL), and cooled to −35 °C. *n*-BuLi (0.09 mL of 1.6 M solution in hexanes, 0.14 mmol, 1.1 equiv) was added dropwise, and the resulting yellow solution was allowed to warm to room temperature while stirring for 0.5 h. In a separate Schlenk flask, $CrCl_2$ (15.0 mg, 0.122 mmol) was suspended in THF (5 mL), followed by the addition of NaCp (0.7 mL of 2.0 M solution in THF, 0.14 mmol, 1.1 equiv); after stirring at room temperature for 0.5 h, the Li[(HIPTNCMe)$_2$CH] prepared above was added. The resulting green to incident and magenta to transmitted light solution was stirred overnight, followed by the removal of the solvent *in vacuo*. The residue was extracted with hexanes and filtered over Celite followed by the addition of pyridine *N*-oxide (12.2 mg, 0.128 mmol, 1.05 equiv), causing the reaction mixture to turn orange over a 5 min period. After stirring overnight at room temperature, the solvent was removed *in vacuo*; the residue was extracted with hexanes, filtered over Celite, concentrated to a volume of approximately 0.5 mL, and cooled to −35 °C to provide a small amount of orange crystalline material (4.5 mg), identified as compound **9** by X-ray crystallography. UV−vis (hexanes; $\lambda_{max}$, nm): 371, 475 (sh).

## ■ ASSOCIATED CONTENT

### Ⓢ Supporting Information

Experimental details for reactions shown in Scheme 3 and attempted catalytic HAT reactions, UV−visible spectra, and crystallographic data for complexes **3**, **4**, **5**, **5a**, **6**, **7**, **8**, **9**. This material is available free of charge via the Internet at http://pubs.acs.org.

## ■ AUTHOR INFORMATION

### Corresponding Author

*E-mail: kevin.m.smith@ubc.ca.

## ■ ACKNOWLEDGMENTS

We are grateful to the Natural Sciences and Engineering Research Council of Canada (NSERC), the Canadian Foundation of Innovation, and the University of British Columbia for financial support. K.M.S. thanks Katherine H. D. Ballem and Julia L. Conway for initial synthesis of complexes **3**, **5**, **5a**, and **7**, Anita Lam for collecting X-ray diffraction data for complexes **6**, **8**, and **9**, Addison N. Desnoyer for preliminary studies of **3** with $Ph_3PI_2$, and Professor Warren E. Piers for helpful discussions.

## ■ REFERENCES

(1) (a) Bolm, C.; Legros, J.; Le Paih, J.; Zani, L. *Chem. Rev.* **2004**, *104*, 6217−6254. (b) Cahiez, G.; Moyeux, A. *Chem. Rev.* **2010**, *110*, 1435−1462. (c) Hu, X. *Chem. Sci.* **2011**, *2*, 1867−1886. (d) Yeung, C. S.; Dong, V. M. *Chem. Rev.* **2011**, *111*, 1215−1292. (e) Sun, C.-L.; Li, B.-J.; Shi, Z.-J. *Chem. Rev.* **2011**, *111*, 1293−1314. (f) Jana, R.; Pathak, T. P.; Sigman, M. S. *Chem. Rev.* **2011**, *111*, 1417−1492. (g) Liu, C.; Zhang, H.; Shi, W.; Lei, A. *Chem. Rev.* **2011**, *111*, 1780−1824.

(2) (a) Poli, R. *Angew. Chem., Int. Ed.* **2006**, *46*, 5058−5070. (b) Smith, K. M.; McNeil, W. S.; Abd-El-Aziz, A. S. *Macromol. Chem. Phys.* **2010**, *211*, 10−16. (c) Poli, R. *Eur. J. Inorg. Chem.* **2011**, 1513−1530.

(3) (a) Chirik, P. J.; Wieghardt, K. W. *Science* **2010**, *327*, 794−795. (b) Smith, A. L.; Hardcastle, K. I.; Soper, J. D. *J. Am. Chem. Soc.* **2010**, *132*, 14358−14360.

(4) (a) Affo, W.; Ohmiya, H.; Fujioka, T.; Ikeda, Y.; Nakamura, T.; Yorimitsu, H.; Oshima, K.; Imamura, Y.; Mizuta, T.; Miyoshi, K. *J. Am. Chem. Soc.* **2006**, *128*, 8068−8077. (b) Jones, G. D.; Martin, J. L.; McFarland, C.; Allen, O. R.; Hall, R. E.; Haley, A. D.; Brandon, R. J.; Konovalova, T.; Desrochers, P. J.; Pulay, P.; Vicic, D. A. *J. Am. Chem. Soc.* **2006**, *128*, 13175−13183. (c) Movassaghi, M.; Schmidt, M. A. *Angew. Chem., Int. Ed.* **2007**, *46*, 3725−3728. (d) Fürstner, A.; Martin, R.; Krause, H.; Seidel, G.; Goddard, R.; Lehmann, C. W. *J. Am. Chem. Soc.* **2008**, *130*, 8773−8787. (e) Li, C.-J. *Acc. Chem. Res.* **2009**, *42*, 335−344. (f) Guo, H.; Dong, C.-G.; Kim, D.-S.; Urabe, D.; Wang, J.; Kim, J. T.; Liu, X.; Sasaki, T.; Kishi, Y. *J. Am. Chem. Soc.* **2009**, *131*, 15387−15393. (g) Spasyuk, D. M.; Zargarian, D.; van der Est, A. *Organometallics* **2009**, *28*, 6531−6540. (h) Gansäuer, A.; Fleckhaus, A.; Lafont, M. A.; Okkel, A.; Kotsis, K.; Anoop, A.; Neese, F. *J. Am. Chem. Soc.* **2009**, *131*, 16989−16999. (i) Nakamura, E.; Yoshikai, N. *J. Org. Chem.* **2010**, *75*, 6061−6067. (j) Zhu, D.; Budzelaar, P. H. M. *Organometallics* **2010**, *29*, 5759−5761. (k) Li, H.; Sun, C.-L.; Yu, M.; Yu, D.-G.; Li, B.-J.; Shi, Z.-J. *Chem.—Eur. J.* **2011**, *17*, 3593−3597. (l) Ren, P.; Vechorkin, O.; von Allmen, K.; Scopelliti, R.; Hu, X. *J. Am. Chem. Soc.* **2011**, *133*, 7084−7095. (m) Dugan, T. R.; Sun, X.; Rybak-Akimova, E. V.; Olatunji-Ojo, O.; Cundari, T. R.; Holland, P. L. *J. Am. Chem. Soc.* **2011**, *133*, 12418−12421. (n) Hatakeyama, T.; Okada, Y.; Yoshimoto, Y.; Nakamura, M. *Angew. Chem., Int. Ed.* **2011**, *50*, 10973−10976. (o) Phillips, A. D.; Thommes, K.; Scopelliti, R.; Gandolfi, C.; Albrecht, M.; Severin, K.; Schreiber, D. F.; Dyson, P. J. *Organometallics* **2011**, *30*, 6119−6132. (p) Weiss, M. E.; Kreis, L. M.; Lauber, A.; Carreira, E. M. *Angew. Chem., Int. Ed.* **2011**, *50*, 11125−11128.

(5) Smith, K. M. *Organometallics* **2005**, *24*, 778−784.

(6) MacLeod, K. C.; Conway, J. L.; Tang, L.; Smith, J. J.; Corcoran, L. D.; Ballem, K. H. D.; Patrick, B. O.; Smith, K. M. *Organometallics* **2009**, *28*, 6798−6806.

(7) MacLeod, K. C.; Patrick, B. O.; Smith, K. M. *Organometallics* **2010**, *29*, 6639−6641.

(8) MacLeod, K. C.; Conway, J. L.; Patrick, B. O.; Smith, K. M. *J. Am. Chem. Soc.* **2010**, *132*, 17325−17334.

(9) (a) Curran, D. P.; Totleben, M. J. *J. Am. Chem. Soc.* **1992**, *114*, 6050−6058. (b) Curran, D. P.; Fevig, T. L.; Jasperse, C. P.; Totleben, M. J. *Synlett* **1992**, 943−961. (c) Curran, D. P.; Gu, X.; Zhang, W.; Dowd, P. *Tetrahedron* **1997**, *53*, 9023−9042. (d) Ogoshi, S.; Stryker, J. M. *J. Am. Chem. Soc.* **1998**, *120*, 3514−3515. (e) Choquette, K. A.; Sadasivam, D. V.; Flowers, R. A. II *J. Am. Chem. Soc.* **2010**, *132*, 17396−17398.

(10) (a) Terao, J.; Saito, K.; Nii, S.; Kambe, N.; Sonoda, N. *J. Am. Chem. Soc.* **1998**, *120*, 11822−11823. (b) Agapie, T.; Diaconescu, P. L.; Mindiola, D. J.; Cummins, C. C. *Organometallics* **2002**, *21*, 1329−1340. (c) Nii, S.; Terao, J.; Kambe, N. *J. Org. Chem.* **2004**, *69*, 573−576. (d) Cossairt, B. M.; Cummins, C. C. *New J. Chem.* **2010**, *34*, 1533−1536. (e) Trunkley, E. F.; Epshteyn, A.; Zavalij, P. Y.; Sita, L. R. *Organometallics* **2010**, *29*, 6587−6593.

(11) Bridging chromium oxo: (a) Di Vaira, M.; Mani, F. *Inorg. Chem.* **1984**, *23*, 409−412. (b) Bottomly, F.; Paez, D. E.; Sutin, L.; White, P. S.; Köhler, F. H.; Thompson, R. C.; Westwood, N. P. C. *Organometallics* **1990**, *9*, 2443−2454. (c) Noh, S.-K.; Heintz, R. A.; Haggerty, B. S.; Rheingold, A. L.; Theopold, K. H. *J. Am. Chem. Soc.* **1992**, *114*, 1892−1893. (d) Ruppa, K. B. P.; Feghali, K.; Kovacs, I.; Aparna, K.; Gambarotta, S.; Yap, G. P. A; Bensimon, C. *J. Chem. Soc., Dalton Trans.* **1998**, 1595−1605. (e) Huang, H.; Rheingold, A. L.; Hughes, R. P. *Organometallics* **2010**, *29*, 3672−3675. (f) O'Reilly, M. E.; Del Castillo, T. J.; Falkowski, J. M.; Ramachandran, V.; Pati, M.; Correia, M. C.; Abboud, K. A.; Dalal, N. S.; Richardson, D. E.; Veige, A. S. *J. Am. Chem. Soc.* **2011**, *133*, 13661−13673.

(12) Terminal chromium oxo: (a) Budge, J. R.; Gatehouse, B. M. K.; Nesbit, M. C.; West, B. O. *J. Chem. Soc., Chem. Commun.* **1981**, 370−371. (b) Groves, J. T.; Kruper, W. J. Jr.; Haushalter, R. C.; Butler, W. M. *Inorg. Chem.* **1982**, *21*, 1363−1368. (c) Morse, D. B.; Rauchfuss, T. B.; Wilson, S. R. *J. Am. Chem. Soc.* **1988**, *110*, 8234−8235. (d) Hess, A.; Hörz, M. R.; Liable-Sands, L. M.; Lindner, D. C.; Rheingold, A. L.; Theopold, K. H. *Angew. Chem., Int. Ed.* **1999**, *38*, 166−168. (e) Odom, A. L.; Mindiola, D. J.; Cummins, C. C. *Inorg. Chem.* **1999**, *38*, 3290−3295. (f) Hess, J. S.; Leelasubcharoen, S.; Rheingold, A. L.; Doren, D. J.; Theopold, K. H. *J. Am. Chem. Soc.* **2002**, *124*, 2454−2455. (g) Qin, K.; Incarvito, C. D.; Rheingold, A. L.; Theopold, K. H. *J. Am. Chem. Soc.* **2002**, *124*, 14008−14009. (h) Mahammed, A.; Gray, H. B.; Meier-Callahan, A. E.; Gross, Z. *J. Am. Chem. Soc.* **2003**, *125*, 1162−1163. (i) Premsingh, S.; Venkataramanan, N. S.; Rajagopal, S.; Mirza, S. P.; Vairamani, M.; Rao, P. S.; Velavan, K. *Inorg. Chem.* **2004**, *43*, 5744−5753. (j) Czernuszewicz, R. S.; Mody, V.; Czader, A.; Gałęzowski, M.; Gryko, D. T. *J. Am. Chem. Soc.* **2009**, *131*, 14214−14215. (k) O'Reilly, M.; Falkowski, J. M.; Ramachandran, V.; Pati, M.; Abboud, K. A.; Dalal, N. S.; Gray, T. G.; Veige, A. S. *Inorg. Chem.* **2009**, *48*, 10901−10903. (l) Groysman, S.; Villagrán, D.; Nocera, D. G. *Inorg. Chem.* **2010**, *49*, 10759−10761. (m) Monillas, W. H.; Yap, G. P. A; Theopold, K. H. *Inorg. Chim. Acta* **2011**, *369*, 103−119.

(13) (a) Qin, K.; Incarvito, C. D.; Rheingold, A. L.; Theopold, K. H. *Angew. Chem., Int. Ed.* **2002**, *41*, 2333−2335. (b) Cho, J.; Woo, J.; Nam, W. *J. Am. Chem. Soc.* **2010**, *132*, 5958−5959. (c) Cho, J.; Woo, J.; Han, J. E.; Kobo, M.; Ogura, T.; Nam, W. *Chem. Sci.* **2011**, *2*, 2057−2062.

(14) (a) Nichols, P. J.; Fallon, G. D.; Moubaraki, B.; Murray, K. S.; West, B. O. *Polyhedron* **1993**, *12*, 2205−2213. (b) Liston, D. J.; Kennedy, B. J.; Murray, K. S.; West, B. O. *Inorg. Chem.* **1985**, *24*, 1561−1567.

(15) Liston, D. J.; West, B. O. *Inorg. Chem.* **1985**, *24*, 1568−1576.

(16) Reagents and experimental details for the reactions illustrated in Scheme 3 can be found in the Supporting Information.

(17) Champouret, Y.; MacLeod, K. C.; Baisch, U.; Patrick, B. O.; Smith, K. M.; Poli, R. *Organometallics* **2010**, *29*, 167−176.

(18) Sun, M.; Mu, Y.; Liu, Y.; Wu, Q.; Ye, L. *Organometallics* **2011**, *30*, 669−675.

(19) (a) Fürstner, A. *Chem.—Eur. J.* **1998**, *4*, 567−570. (b) Fürstner, A. *Pure Appl. Chem.* **1998**, *70*, 1071−1076.

(20) Fürstner, A.; Hupperts, A. *J. Am. Chem. Soc.* **1995**, *117*, 4468−4475.

(21) Fürstner, A.; Shi, N. *J. Am. Chem. Soc.* **1996**, *118*, 12349−12357.

(22) Fernández-Zúmel, M. A.; Buron, C.; Severin, K. *Eur. J. Org. Chem.* **2011**, 2272−2277.

(23) Bandini, M.; Cozzi, P. G.; Umani-Ronchi, A. *Chem. Commun.* **2002**, 919−927.

(24) Gansäuer, A.; Bluhm, H.; Pierobon, M. *J. Am. Chem. Soc.* **1998**, *120*, 12849−12859.
(25) Shaughnessy, K. H.; Huang, R. *Synth. Commun.* **2002**, *32*, 1923−1928.
(26) Namba, K.; Kishi, Y. *Org. Lett.* **2004**, *6*, 5031−5033.
(27) Wessjohann, L. A.; Scheid, G. *Synthesis* **1999**, 1−36.
(28) Hansen, K. B.; Leighton, J. L.; Jacobsen, E. N. *J. Am. Chem. Soc.* **1996**, *118*, 10924−10925.
(29) The Cr(III) enolate compound was previously reported: Champouret, Y.; MacLeod, K. C.; Smith, K. M.; Patrick, B. O.; Poli, R. *Organometallics* **2010**, *29*, 3125−3132.
(30) $MnI_2$ was prepared in situ by stirring $I_2$ with excess Mn powder in THF, followed by filtration over Celite to remove unreacted Mn powder.
(31) McGarrigle, E. M.; Gilheany, D. G. *Chem. Rev.* **2005**, *105*, 1563−1602.
(32) Scott, S. L.; Bakac, A.; Espenson, J. H. *J. Am. Chem. Soc.* **1991**, *113*, 7787−7788.
(33) (a) Mayer, J. M. *Acc. Chem. Res.* **1998**, *31*, 441−450. (b) Gunay, A.; Theopold, K. H. *Chem. Rev.* **2010**, *110*, 1060−1081. (c) Warren, J. J.; Tronic, T. A.; Mayer, J. M. *Chem. Rev.* **2010**, *110*, 6961−7001. (d) Mayer, J. M. *Acc. Chem. Res.* **2011**, *44*, 36−46.
(34) (a) Bakac, A.; Espenson, J. H. *Acc. Chem. Res.* **1993**, *26*, 519−523. (b) Bakac, A. *J. Am. Chem. Soc.* **2000**, *122*, 1092−1097. (c) Bakac, A. *Inorg. Chem.* **2010**, *49*, 3584−3593.
(35) Levina, A.; Lay, P. A. *Coord. Chem. Rev.* **2005**, *249*, 281−298.
(36) (a) King, A. R.; Hennessy, E. T.; Betley, T. A. *J. Am. Chem. Soc.* **2011**, *133*, 4917−4923. (b) Cowley, R. E.; Eckert, N. A.; Vaddadi, S.; Figg, T. M.; Cundari, T. R.; Holland, P. L. *J. Am. Chem. Soc.* **2011**, *133*, 9796−9811. (c) Bowman, A. C.; Milsmann, C.; Bill, E.; Turner, Z. R.; Lobkovsky, E.; DeBeer, S.; Wieghardt, K.; Chirik, P. J. *J. Am. Chem. Soc.* **2011**, *133*, 17353−17369.
(37) Dzik, W. I.; Vlugt, J. I. v. d.; Reek, J. N. H.; de Bruin, B. *Angew. Chem., Int. Ed.* **2011**, *50*, 3356−3358.
(38) Lu, A.; Zhang, X. P. *Chem. Soc. Rev.* **2011**, *40*, 1899−1909.
(39) (a) Knijnenburg, Q.; Gambarotta, S.; Budzelaar, P. H. M. *Dalton Trans.* **2006**, 5442−5448. (b) Zhu, D.; Thapa, I.; Korobkov, I.; Gambarotta, S.; Budzelaar, P. H. M. *Inorg. Chem.* **2011**, *50*, 9879−9887.
(40) (a) Yandulov, D. V.; Schrock, R. R. *Science* **2003**, *301*, 76−78. (b) Schrock, R. R. *Acc. Chem. Res.* **2005**, *38*, 955−962. (c) Yandulov, D. V.; Schrock, R. R. *Inorg. Chem.* **2005**, *44*, 1103−1117, [erratum p 5542]. (d) Byrnes, M. J.; Dai, X.; Schrock, R. R.; Hock, A. S.; Müller, P. *Organometallics* **2005**, *24*, 4437−4450. (e) Smythe, N. C.; Schrock, R. R.; Müller, P.; Weare, W. W. *Inorg. Chem.* **2006**, *45*, 7111−7118.
(41) Kenward, A. L.; Ross, J. A.; Piers, W. E.; Parvez, M. *Organometallics* **2009**, *28*, 3625−3628, [erratum p 4898].
(42) (a) Hiyama, T.; Sawahata, M.; Obayashi, M. *Chem. Lett.* **1983**, 1237−1238. (b) Estévez, R. E.; Justicia, J.; Bazdi, B.; Fuentes, N.; Paradas, M.; Choquesillo-Lazarte, D.; García-Ruiz, J. M.; Robles, R.; Gansäuer, A.; Cuerva, J. M.; Oltra, J. E. *Chem.—Eur. J.* **2009**, *15*, 2774−2791.
(43) (a) Quebatte, L.; Thommes, K.; Severin, K. *J. Am. Chem. Soc.* **2006**, *128*, 7440−7441. (b) Thommes, K.; Içli, B.; Scopelliti, R.; Severin, K. *Chem.—Eur. J.* **2007**, *13*, 6899−6907. (c) Pintauer, T.; Matyjaszewski, K. *Chem. Soc. Rev.* **2008**, *37*, 1087−1097. (d) Pintauer, T. *Eur. J. Inorg. Chem.* **2010**, 2449−2460. (e) Thommes, K.; Fernández- Zúmel, M. A.; Buron, C.; Godinat, A.; Scopelliti, R.; Severin, K. *Eur. J. Org. Chem.* **2011**, 249−255.
(44) Champouret, Y.; Baisch, U.; Poli, R.; Tang, L.; Conway, J. L.; Smith, K. M. *Angew. Chem., Int. Ed.* **2008**, *47*, 6069−6072.
(45) Doherty, J. C.; Ballem, K. H. D.; Patrick, B. O.; Smith, K. M. *Organometallics* **2004**, *23*, 1487−1489.
(46) Brown, J. L.; Wu, G.; Hayton, T. W. *J. Am. Chem. Soc.* **2010**, *132*, 7248−7249, and references therein.
(47) (a) Baker, M. V.; Field, L. D.; Hambley, T. W. *Inorg. Chem.* **1988**, *27*, 2872−2876. (b) Schubert, E. M. *J. Chem. Educ.* **1992**, *69*, 62.
(48) *SAINT*, version 7.46A; Bruker Analytical X-ray System: Madison, WI, 1997−2007.
(49) *SADABS: Bruker Nonius area detector scaling and absorption correction*, V. 2.10; Bruker AXS Inc.: Madison, WI, 2003.
(50) (a) *SIR97*. Altomare, A.; Burla, M. C.; Cammalli, G.; Cascarano, M.; Giacovazzo, C.; Guagliardi, A.; Moliterni, A. G. G.; Polidori, G.; Spagna, A. *J. Appl. Crystallogr.* **1999**, *32*, 115−119. (b) *SIR92*. Altomare, A.; Cascarano, G.; Giacovazzo, C.; Guagliardi, A. *J. Appl. Crystallogr.* **1993**, *26*, 343−350.
(51) *SHELXTL*, Version 5.1; Bruker AXS Inc.: Madison, WI, 1997.
(52) Farrugia, L. J. *J. Appl. Crystallogr.* **1997**, *32*, 565.
(53) *SQUEEZE*. Sluis, P. v. d.; Spek, A. L. *Acta Crystallogr.* **1990**, *A46*, 194−201